

## SUPPLEMENTAL MATERIAL

Çetiner et al., <https://doi.org/10.1085/jgp.201611699>

### Intensity of light scattering by bacterial suspension

Light scattering is a flexible tool with excellent time resolution that allows us to observe the time course of bacterial responses to osmotic stresses. The directional intensity of the scattered light depends on multiple factors, including the experimental setup, the shape of bacterial cells, and the cytoplasmic composition. For a suspension of EC, light scattering can be described by the Rayleigh–Gans approximation (Koch et al., 1996):

$$I = \frac{8\pi^4 r^6 \eta_0^4}{R^2 \lambda^4} \cdot \frac{\left[\left(\frac{\eta}{\eta_0}\right)^2 - 1\right]^2}{\left[\left(\frac{\eta}{\eta_0}\right)^2 + 2\right]^2} \cdot \nu I_0 V [1 + \cos^2(\theta)] \cdot P(\theta), \quad (\text{S1})$$

where  $I$  is the intensity of the scattered light for a given direction and distance,  $r$  is the radius of the spherical equivalent of the actual particle (in our case, a rod-shaped bacterium),  $\eta_0$  is the index of refraction of the suspending medium,  $\eta$  is the index of refraction of the particle,  $V$  is the volume illuminated,  $I_0$  is the intensity of the incident light,  $\nu$  is the concentration of particles,  $\theta$  is the angle of observation,  $R$  is the distance of the detector from the sample, and  $\lambda$  is the wavelength of light in vacuum. The factor  $[1 + \cos^2(\theta)]$  depends on the angle of observation,  $\theta$ , relative to the forward direction of the illuminating beam. For a given physical setup, most of these factors can be combined into an empirical constant.  $P(\theta)$  is a correction function that compensates for the light interference within the particle and depends on the geometry of the scattering particle. For an ellipsoid of revolution, it is approximated as

$$P(\theta) = (3(\sin x - x \cos x) / x^3)^2, \quad (\text{S2})$$

where

$$x = \left(\frac{4\pi a}{\lambda}\right) \left(\sin \frac{\theta}{2}\right) \left(\sin^2 \beta + \left(\frac{b}{a}\right)^2 \cos^2 \beta\right)^{\frac{1}{2}}, \quad (\text{S3})$$

$\beta$  is the angle of orientation of the ellipsoid of revolution to the direction of the light beam,  $a$  is the rotation radius of ellipsoid, and  $b/a$  is the ratio of the major to minor axis (Koch et al., 1996). To determine the amount of scattered light falling onto the detector, the equation with the substitutions should be integrated over the angular range covered by the detector and averaged over random orientations ( $\beta$  angles) of the ellipsoids in 3D space.

To enable quantitative estimation of the bacterial properties from the scattering traces, the intensity equation needs to be configured to match the specific parameters of the experimental setup (e.g., scattering angle, distance, amplification, background reflected lighting, etc.; Koch et al., 1996; Foladori et al., 2008).

According to Eqs. S1–S3, the intensity of scattering is a function of several parameters characterizing the geometric and optical properties of the bacteria, primarily the size and the refraction index. The refraction index of a bacterium depends on the concentration and nature of solutes in the cytoplasm. For our purpose of studying the role of MscS in bacterial response to hypoosmotic shock, all molecular species can be divided into two broad categories: permeable (ions and other low-molecular-weight solutes that can exit through MscS or MscL) and impermeable (proteins, nucleic acids, etc.). It has been shown (Craig et al., 1995; Ball and Ramsden, 1998) that contributions of both small solutes and macromolecules to the refraction index of a solution scale linearly with their concentrations. If the bacterial cytoplasm is approximated as a uniform solution of all internal components, its refraction index can be estimated as

$$\eta = \eta_w + \frac{d\eta}{dC_p} C_p + \frac{d\eta}{dC_i} C_i = \eta_w + \left(\frac{d\eta}{dC_p} m_p + \frac{d\eta}{dC_i} m_i\right) / V_c, \quad (\text{S4})$$

where  $\eta$  is the refraction index of the cytoplasm,  $\eta_w$  refraction index of water,  $C_p$  and  $m_p$  are the concentration and total mass of the permeable species,  $C_i$  and  $m_i$  are those of impermeable species in the solution, respectively, and  $V_c$  is the total volume of the bacterial cytoplasm.

Because the purpose of the current study is to estimate membrane permeability during osmotic shock, here we focus on the time course of the relative change in the cytoplasm volume and internal content rather than absolute quantification of the optical properties. From this viewpoint, the equation for the intensity of the captured scattered light can be rewritten to separate the terms that are essentially constant from the time-dependent variables:

$$I_r = I_b + A r^6 \cdot \frac{\left[ \left( \frac{\eta_w + 3(S_p m_p + S_i m_i) / 4\pi r^3}{\eta_0} \right)^2 - 1 \right]^2}{\left[ \left( \frac{\eta_w + 3(S_p m_p + S_i m_i) / 4\pi r^3}{\eta_0} \right)^2 + 2 \right]^2}. \quad (\text{S5})$$

Here,  $I_r$  is the intensity of the recorded scattered light,  $I_b$  is the background light component,  $r$  is the radius of the spherical equivalent of the bacterium,  $\eta_w$  is the refraction index of water,  $\eta_0$  is the refraction index of extracellular medium,  $m_p$  and  $m_i$  are the masses of the permeable and impermeable solutes, respectively,  $S_p$  and  $S_i$  are the scaling coefficients between their concentrations and contributions to the refraction index of the medium ( $S_p = d\eta/dC_p$ ,  $S_i = d\eta/dC_i$ ; see Eq. S4), and  $A$  is the scaling coefficient for the amplitude of the scattered light that combines components for the instrumental amplification ( $A_i$ ), system geometry, angular dependence (should be integrated over the range of detection angles), light intensity, etc. (notation as in Eq. S1):

$$A = A_i \frac{8\pi^4 \eta_0^4}{R^2 \lambda^4} \cdot \nu I_0 V \int_{\theta_{min}}^{\theta_{max}} P(\theta) [1 + \cos^2(\theta)] \sin(\theta) d\theta. \quad (\text{S6})$$

Strictly speaking, the parameter  $P(\theta)$  under the integral is time-dependent as it includes the axial parameters of bacterial shape (see Eqs. S2 and S3), which may change during the osmotic response (swelling/shrinkage). However, considering the light detector we use, since the relatively dense suspension of bacteria causes multiple scattering events and smearing of the angular intensity peaks, the integrated value for the angular dependence should not change significantly with time.

During the osmotic down-shock, two of the variables in Eq. S5 will undergo quick changes: the effective radius of the bacterium ( $r$ ) and the mass of permeable osmolytes that are confined within the cells ( $m_p$ ). The rest of the entries in the equation can be considered nearly constant. Soon after mixing/dilution, bacteria swell and reach their maximum size; after that moment, the cell geometry remains relatively stable. Although osmolytes are escaping through MS channels, the changes in the scattered light intensity are defined mostly by the mass of permeable osmolytes remaining inside the cell. Light scattering at this point is roughly proportional to the square of solute mass inside the cell. In the case of moderate osmotic shrinking (osmolytes remain in the cell while water is being lost), the intensity of light scattering scales as  $(1/r^2)$ , i.e., inverse to the cell surface area) or as volume to the power of  $-2/3$  (Koch, 1961).

The above analysis indicates that in the course of osmolyte efflux the refractive index difference between the cell and its environment is the major parameter and has a strong dependence on time. Under the assumption that the cell volume changes are small, the time course of the scattering signal can be presented in the following form:

$$I = I_0 + S(m_i + m_p(t))^2,$$

where  $I$  is light intensity,  $I_0$  is background light intensity,  $S$  is scaling coefficient,  $m_i$  is the mass of impermeable osmolytes, and  $m_p(t)$  is the mass of permeable osmolytes as a function of time  $t$ . Under the assumption that the efflux is proportional to the internal concentration (under the conditions of much lower external osmolarity)

$$\frac{dm_p}{dt} = -\frac{m_p}{\tau},$$

we may define  $\tau$  as the time constant of the permeable osmolyte release.

$$\frac{dm_p}{m_p} = -\frac{dt}{\tau}$$

$$\int \frac{1}{m_p} dm_p = \int -\frac{1}{\tau} dt$$

$$\ln m_p - \ln m_{p0} = -\frac{t}{\tau} + \frac{t_0}{\tau},$$

where  $m_{p0}$  is the initial mass of the permeable osmolytes before the release and  $t_0$  is the time at which the exponential release has started.

$$m_p = m_{p0} e^{\frac{t_0-t}{\tau}}$$

$$I = I_0 + S(m_i + m_{p0} e^{\frac{t_0-t}{\tau}})^2.$$

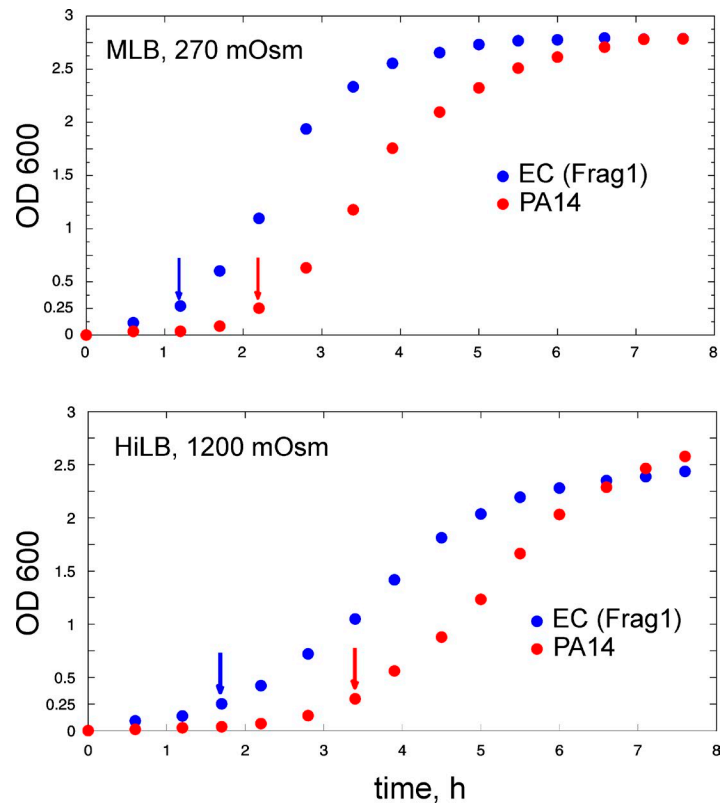


Figure S1. **The growth kinetics of EC (Frag-1) and PA14 in low-osmotic and high-osmotic media.** Standard overnight cultures of EC and PA grown in LB were diluted 1:100 (0.2 ml into 20 ml) into either MLB (270 mOsm; top) or HiLB (1,200 mOsm; bottom). Measurements were performed on a Jasco V-550 double-beam spectrophotometer with 1-cm cuvettes. By the eighth hour, both cultures reached OD<sub>600</sub> of 2.5–2.7. The arrows indicate OD<sub>600</sub> of 0.25, representing the early logarithmic phase of cultures used in all experiments.

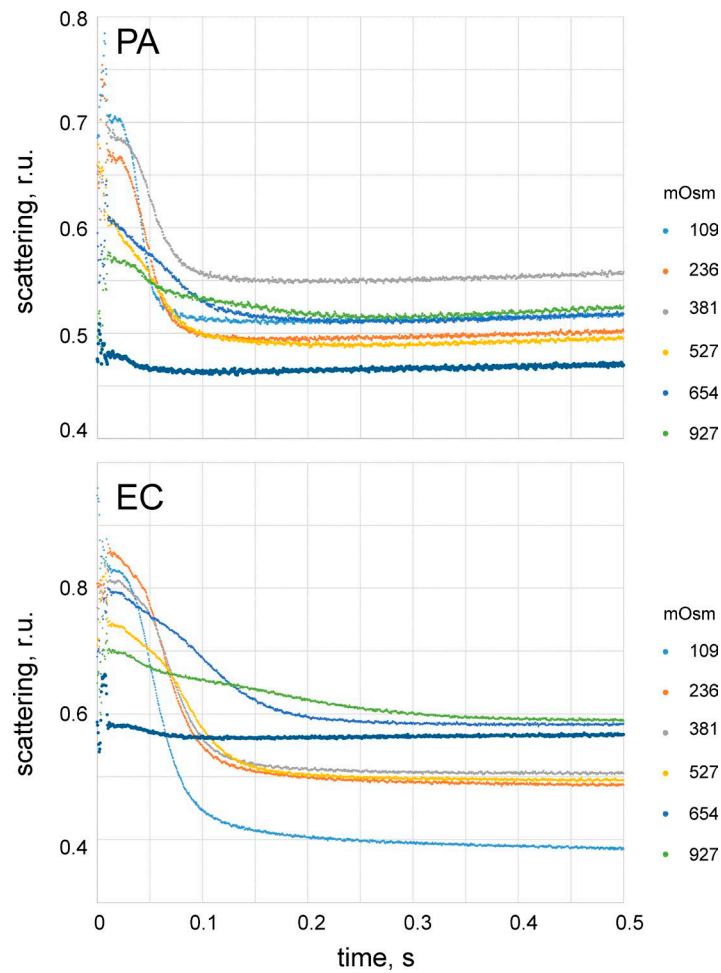
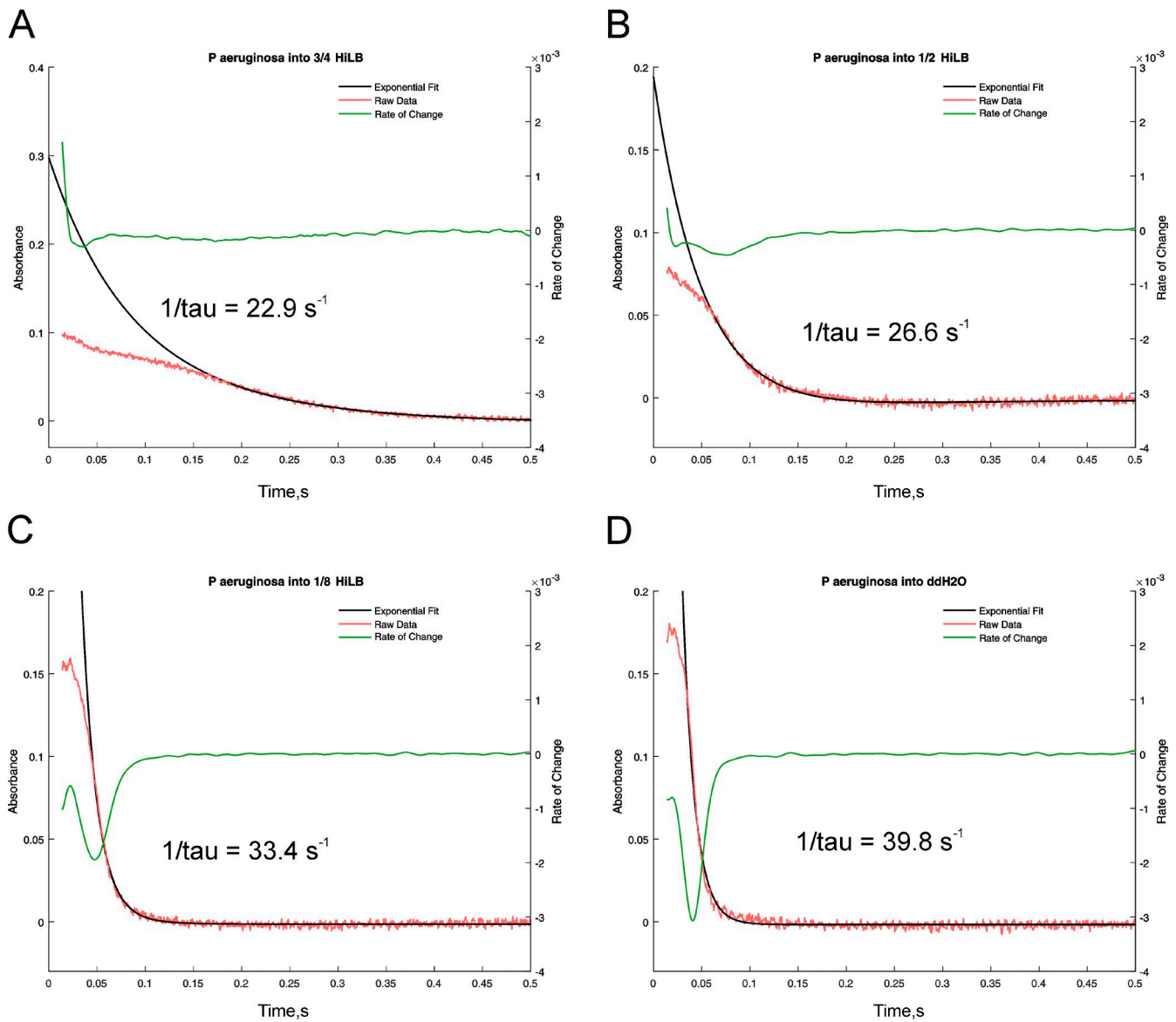
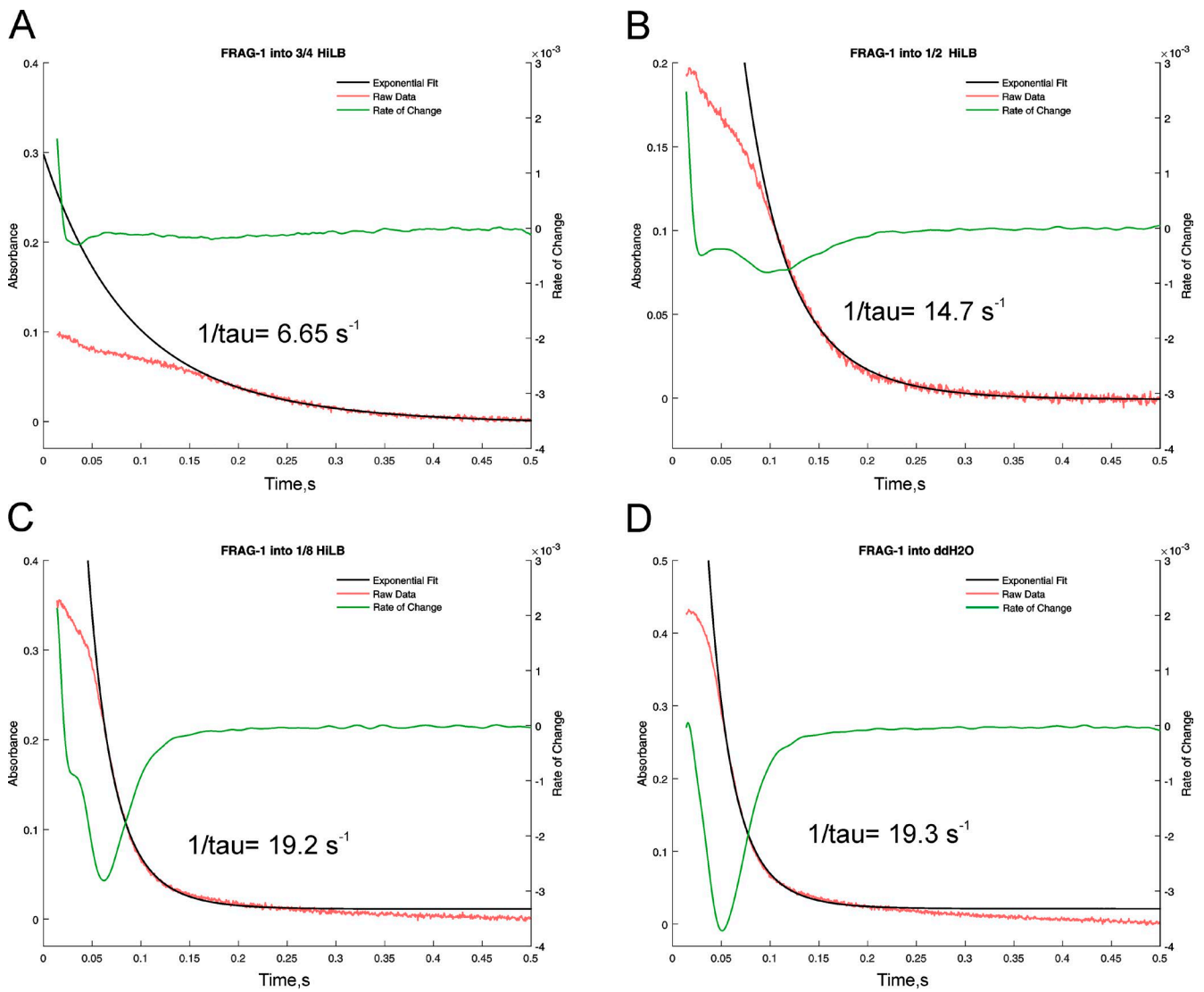


Figure S2. **Unadjusted stopped-flow scattering traces obtained after subtraction of stray light signals.** Initially, the cultures were grown in HiLB (1,200 mOsm) to  $OD_{600}$  of 0.25, concentrated to  $OD_{600}$  of 2.2, and then subjected to various down-shocks in the stopped-flow machine. The scattering is presented in relative units (r.u.) corresponding to the output voltage from the photomultiplier. On the right, values of endpoint osmolarities are shown with color code for respective traces. The dark blue line represents the no-shock mixing control. The top and bottom graphs show experiments with PA-14 and Frag-1 strains, respectively. The deviation of no-shock (control) traces from a straight line reflect possible response to shear stress.



$$I0 + S*(mi + mp * \exp((t0 - t)/\tau))^2$$

Figure S3. Scattering traces fitted with the modified Rayleigh-Gans equation combined with an exponential release kinetics. (A–D) Examples of fitting curves (black) overlaid with experimental traces (red) obtained with PA-14 cultures shocked from HiLB to 3/4 HiLB (A), 1/2 HiLB (B), 1/8 HiLB (C), and distilled water (D). To obtain a maximal rate of release, fitting in most cases started at the point of steepest downfall designated by the minimum of a first derivative (green). Before fitting, the traces were adjusted such that at  $t = 0.5$  s the scattering signal was zero. Fitting was performed in MATLAB using the equation at the bottom.



$$I_0 + S \cdot (m_i + m_p \cdot \exp(-(t_0 - t)/\tau))^2$$

Figure S4. **Scattering traces fitted with the modified Rayleigh-Gans equation.** (A–D) Examples of fitting curves (black) overlaid with experimental traces (red) obtained with EC (Frag-1) cultures shocked from HiLB to 3/4 HiLB (A), 1/2 HiLB (B), 1/8 HiLB (C), and distilled water (D). As previously, fitting in most cases started at the point of steepest downfall designated by the minimum of a first derivative (green). In contrast to PA, a slow component was observed in EC traces as deviation between the experimental and fitting curves.

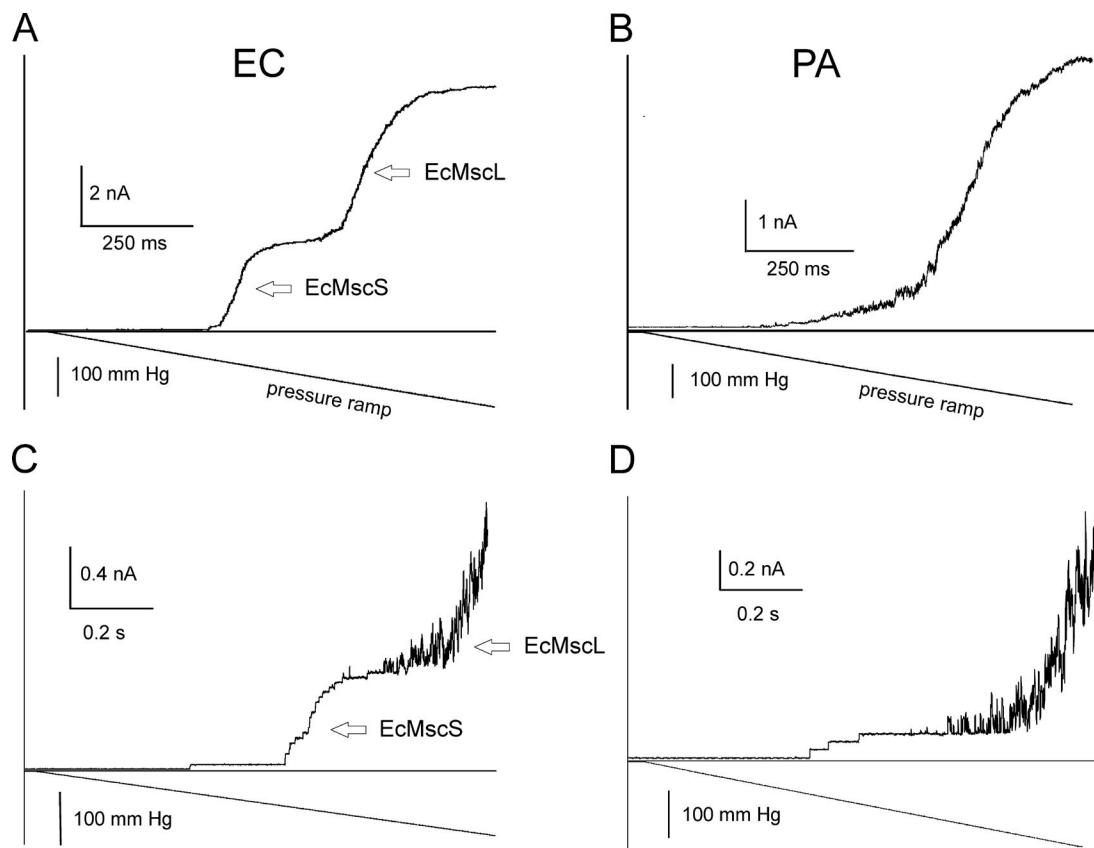


Figure S5. **The examples of ramp responses in representative patches from EC and PA spheroplasts.** (A–D) Pressure ramps applied to excised patches of EC (A and C) always reveal a larger MscS population as compared with PA (B and D). In the latter case, it is not always possible to count individual channels, as the current raises gradually and shows no obvious two-wave character. The traces in C and D represent clear cases when the MscS- and MscL-like channels can be easily separated and counted. 12 successful patches from PA and 9 patches from the Frag-1 strain permitted quantification of channel density in these organisms (Table 1).

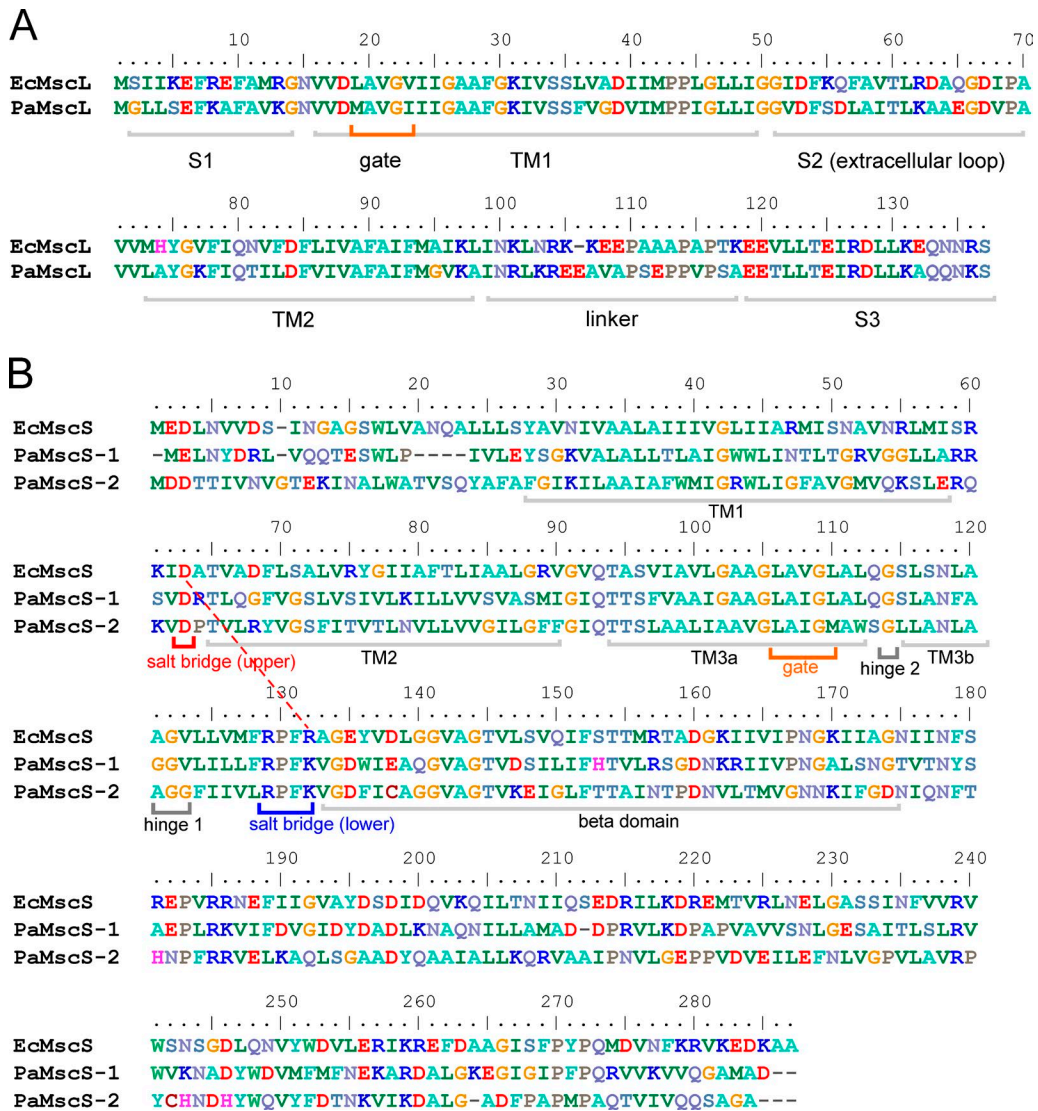


Figure S6. Alignments of EC and PA MS channel orthologues. (A) Full sequence alignments of EcMscL and PaMscL. (B) Partial alignment of the core transmembrane segments of EcMscS with two PaMscS species, including the N-terminal part of the cage  $\beta$  domain. The sequences predict the same position of the hydrophobic gate, salt bridges responsible for interdomain interactions, and all elements involved in inactivation, including double glycine motifs that made TM3 hinges (hinge 1) even more flexible than in EcMscS.



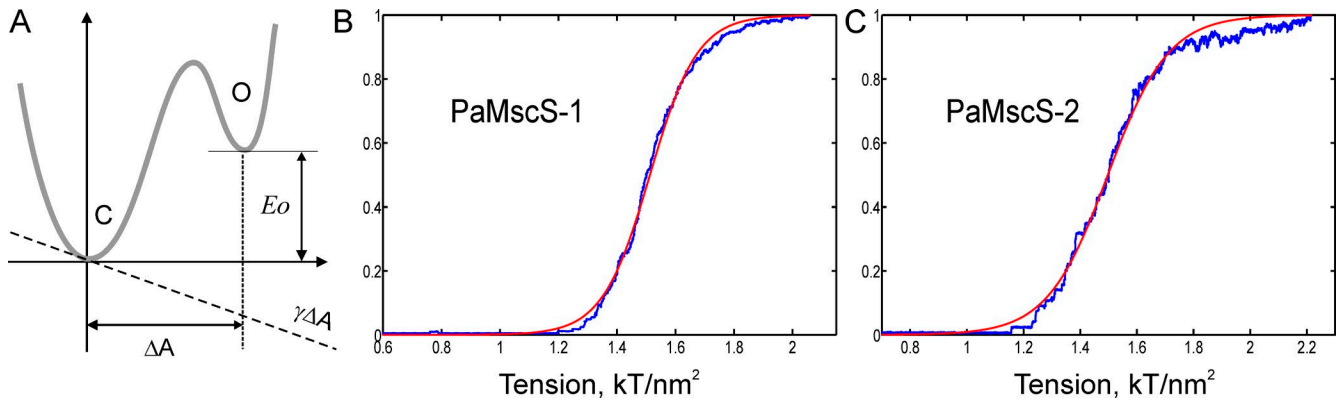


Figure S7. **Determination of the spatial and energetic parameters of channel gating from dose-response curves.** (A) A two-state energy diagram for tension-gated channel. (B and C) Open probabilities ( $P_o$ ) plotted as a function of tension ( $\text{kT}/\text{nm}^2$ ) for PaMscS-1 (B) and PaMscS-2 (C).  $P_o$  was fitted to two state Boltzmann function  $P_o = 1/(1 + \exp((\Delta E - \gamma\Delta A)/kT))$ , and gating parameters were extracted from the fits (red curves). The parameters of energy  $\Delta E$  and in-plane expansion  $\Delta A$  are shown in Table 2.

Table S1. **PA PA-14 putative proteins homologous to known MS channel proteins of EC**

EC protein	Length of EC protein (aa)	Closest PA orthologue	Predicted length of PA protein (aa)	Percent identity (BLAST)
MscL	136	PA14_61050 (PaMscL)	137	64
MscS	286	PA14_57110 (PaMscS-1)	278	36
		PA14_65040 (PaMscS-2)	283	29
KefA/MscK	1,120	PA14_66400	1,118	40
YbdG	415	PA14_19230	442	44
YbiO	741	PA14_67630	735	33
YjeP	1,107	PA14_46240	807	35
YnaI	343	No homologue	-	-

MscS has two homologues of comparable length designated as PaMscS-1 and PaMscS-2. MscK aligns well with a single putative “long MscS-family” protein PA\_66400 (1,118 residues). YjeP, which is an orthologue of MscK in EC, also aligns with PA\_66400, but the alignment with MscK is better. A shorter putative 807-residue protein, PA14\_46240, aligns with YjeP with a 35% identity in the characteristic MscS region. YnaI does not seem to have a direct homologue in PA-14.

## REFERENCES

- Ball, V., and J.J. Ramsden. 1998. Buffer dependence of refractive index increments of protein solutions. *Biopolymers*. 46:489–492. [http://dx.doi.org/10.1002/\(SICI\)1097-0282\(199812\)46:7<489::AID-BIP6>3.0.CO;2-E](http://dx.doi.org/10.1002/(SICI)1097-0282(199812)46:7<489::AID-BIP6>3.0.CO;2-E)
- Craig, J.P., P.A. Simmons, S. Patel, and A. Tomlinson. 1995. Refractive index and osmolality of human tears. *Optom. Vis. Sci.* 72:718–724.
- Foladori, P., A. Quaranta, and G. Ziglio. 2008. Use of silica microspheres having refractive index similar to bacteria for conversion of flow cytometric forward light scatter into biovolume. *Water Res.* 42:3757–3766. <http://dx.doi.org/10.1016/j.watres.2008.06.026>
- Koch, A.L. 1961. Some calculations on the turbidity of mitochondria and bacteria. *Biochim. Biophys. Acta.* 51:429–441. [http://dx.doi.org/10.1016/0006-3002\(61\)90599-6](http://dx.doi.org/10.1016/0006-3002(61)90599-6)
- Koch, A.L., B.R. Robertson, and D.K. Button. 1996. Deduction of the cell volume and mass from forward scatter intensity of bacteria analyzed by flow cytometry. *J. Microbiol. Methods.* 27:49–61. [http://dx.doi.org/10.1016/0167-7012\(96\)00928-1](http://dx.doi.org/10.1016/0167-7012(96)00928-1)